Superfluorescence without inversion in coherently driven three-level systems

Victor Kozlov,* Olga Kocharovskaya, Yuri Rostovtsev, and Marlan Scully
Department of Physics, Texas A&M University, College Station, Texas 77843
(Received 1 March 1999)

A superfluorescence effect in a V-type medium with initial Raman inversion, driven by a strong coherent field on one of the transitions, is studied analytically and numerically. It is shown that the collective spontaneous emission evolves in the presence of a minor population of an upper state of a superfluorescent transition. In the limit of the Rabi frequency of a driving field large compared to that of a superfluorescent pulse, the system of two equations for the fields and density-matrix equations for three states of the medium is reduced to Maxwell-Bloch equations for an effective two-level system. The shape of a superfluorescent pulse is perfectly described in terms of a slowly varying envelope function (which is a solution of the Maxwell-Bloch equations), filled with fast oscillations associated with Rabi floppings on the driving transition. In the average, i.e., after integrating over a period of Rabi oscillations, the upper superfluorescent state is populated less than other states, such that the phenomenon may be called ''superfluorescence without inversion'' by analogy with lasing without inversion. [S1050-2947(99)04408-X]

PACS number(s): 42.50.Gy, 42.50.Fx, 42.65.Re

I. INTRODUCTION

In recent years there have been many intriguing theoretical and experimental proposals for manipulating some of the coherence effects in atomic systems to achieve amplification of a weak probe beam without requiring a traditional population inversion among the bare states of the medium. These proposals, several of which are discussed in Ref. [1], have been broadly classified as ''lasing without inversion'' (LWI) and have created a great deal of interest because of their potential for generating laser light at regions of the electromagnetic spectrum where it is currently difficult or impossible to do so. However, any laser system in the x-ray region meets with difficulties in the design of the reflecting mirrors, which do not permit use of the usual stimulated radiation process for the generation of coherent radiation. From this point of view the spontaneous radiative decay of an ensemble of atoms or molecules in the collective mode, known as superfluorescence, is the optimal process for extracting coherent energy from an inverted mirrorless system. However, we again come to the requirement of population inversion on the radiative transition. In such a situation, a possible way to create the mirrorless source of optical coherent high-frequency radiation lies in the combination of LWI physics together with the superfluorescence effect. This concept of ''superfluorescence without inversion'' is embodied in a realistic three-level atomic configuration of the V type and is investigated in detail in the present paper.

Before we proceed let us make more certain the usage of two different terms—*superfluorescence* and *superradiance*. The superradiance concept for N spin-$\frac{1}{2}$ systems (which are equivalent to two-level atoms), placed in a volume of less than optical wavelength, has been developed by Dicke in his classic paper [2]. He showed the existence of superradiant states, with the decay rate scaled as N^2, and a subradiant state that never decays. As an example, he considered a simple system of two neutrons in a uniform magnetic field, one being in the excited spin state and the other in the ground state. He pointed out that the triplet or symmetric superposition state of one excited and one unexcited state has the double radiation rate of a single excited neutron (superradiance). On the other hand, the singlet or antisymmetric state never decays (subradiance).

The main point is how to prepare an ensemble of two-level atoms in the superradiant state. One possible way is to use a coherent pulse of external radiation. In this case a coherent superposition of upper and lower states for each atomic dipole (spin) will be automatically prepared, implying the inducing of phase correlations between all dipoles in the ensemble. The emission time of this collective dipole is N times faster than the decay time of a single dipole, and this collective decay is known as free induction decay.

Another possibility that seems much more interesting is to use an incoherent pumping pulse, which prepares an ensemble of N atoms in some incoherent mixture of upper and lower states. The whole process, which starts from small quantum fluctuations, with the subsequent self-organization of atoms and their collective spontaneous emission, and which finally results in a pulse with a duration shorter than the decay time of a single dipole, is called superfluorescence (SF). This effect is due to the induction of correlations between the dipole moments of the spatially separated atoms interacting via a common electromagnetic field. For this self-organization process, population inversion is required as a source of instability, providing growth in coherent polarization, and the rate of this instability is proportional to the total population inversion. As a result, the atoms in a volume of a macroscopic size emit coherently. Since the total energy radiated by an ensemble of N inverted atoms is $N\hbar\omega_{ab}$, where ω_{ab} is the transition frequency, then the emission intensity can scale as $I \propto N^2$.

Since Dicke's paper, there has been some work done on superradiance and subradiance in three-level systems [3–5], including a paper by Keitel, Scully, and Sussmann on three-

*Present address: Department of Physics, University of Rochester, Rochester, NY 14627-0771.

level superradiance in the V configuration [5], where it was shown how microwave pulses resonant with one transition can produce and destroy a superradiant state at the other optical transition. This result as well as the fact that the net gain in the three-level driven system may occur without need of population inversion [1] allow us to expect that population inversion at the operating transition should not be necessary for the realization of superfluorescence in three-level atoms coherently driven at the adjacent transition. This is due to the strong influence of the coherent driving field on the interference processes in three-level atoms. The possibility of SF without inversion is exactly the problem we address in this paper.

The SF phenomenon manifests itself also in the Raman scattering of light (cooperative Raman scattering) and has been observed by Pivtsov *et al.* [6] in molecular hydrogen. In [7] it has been shown that the time-dependent scattering dynamics of a quasimonochromatic pulse is very similar to the collective spontaneous emission from two-level atoms with the dipole moment lowered by a factor of Ω/Δ, where Ω and Δ are the Rabi frequency and the detuning of the scattered field. Generally, Raman schemes require high-intensity pump fields, because they operate at large values of detunings, where the atom-field interaction is weak. Approaching the resonance, i.e., taking into consideration a third level that is resonantly coupled to the other two, allows one to diminish dramatically the requirement on the pump intensity and gives rise to the new interesting phenomena. Thus, in [8] the effect of resonant spontaneous cooperative Raman scattering has been considered in the three-level atomic system of a Λ configuration, when the incident field excites the atoms from the lower to the upper level, creating the population inversion between the upper and the intermediate (initially unpopulated) levels. If the excitation and the scattering processes are fast enough to prevent phase relaxation from destroying atomic coherence, the atomic dipoles that oscillate at the scattering frequency retain their phase memory and therefore they radiate cooperatively.

More recent work [9] contains an extension of the concept of amplification without inversion to the SF problem for a particular Λ configuration. Two lower levels of the three-level system are closely spaced, so that the spectrum of the SF pulse covers them both. It has been demonstrated that SF can take place without the need of population inversion if atoms have been initially prepared in a certain coherent superposition of the lower states, and some ways for preparing these states are discussed.

For generation of the coherent radiation in the high-frequency region preference is given to the up-conversion schemes, where the low-frequency photons are converted to those of high-frequency. From this standpoint a three-level system where two fields are coupled through the lower level (V-type medium), see Fig. 1, turns out to be the most advantageous. This system possesses gain without population inversion for the probe field, even with a minor population of the upper level (LWI gain). Stimulated emission of LWI systems has been discussed in numerous papers, while cooperative spontaneous emission is less well understood. In particular, LWI gain appears only for systems with specific relationships between decay constants, while a SF pulse has to evolve on a time scale shorter than all decays, since the

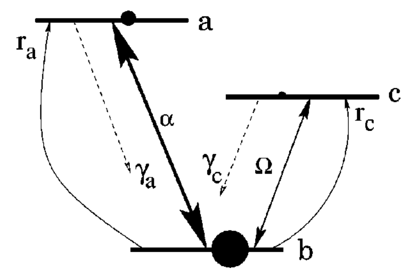

FIG. 1. Level scheme of the V-type medium showing the coherent driving (Ω) and laser (α) fields, decays γ_a, γ_c, and incoherent pump rates r_a, r_c. Circles illustrate the relative initial distribution of populations between the levels in a medium with Raman inversion.

relaxation processes may destroy the phase interatomic correlations. So, it is not clear *a priori* what kind of gain one should expect for the SF system.

Indeed, our numerical calculations prove that a SF pulse has to be shorter than all decay processes in the system, and hence LWI gain in its ordinary sense has no time to develop. However, we show that the conventional definition of gain without inversion might be extended for ultrafast coherent phenomena, such that the LWI condition is asserted ''in the average,'' i.e., after averaging over the period of Rabi oscillations on the driving transition.

Taking into account that the duration of a SF pulse is shorter than all relaxation times, we can considerably simplify the treatment by omitting all relaxation terms in the density-matrix equations. Then, using the given driving-field approximation we reduce the system of coupled equations for six density-matrix elements to the familiar system of two Bloch-like equations. The latter describes the interaction of the field with an effective (pseudo) two-level system. This new two-level system does not constitute a real atomic situation, but appears as the mathematical result of the reduction of the original equations. Formally speaking, we have found a convenient basis in which the complex picture of the interaction of two fields with two coupled optical transitions shows up as an interaction of a probe field with a single optical transition.

The reduction of the original density-matrix equations for a three-level system to the Bloch-type equations becomes possible due to the separation of the fast oscillations of the field and atomic variables associated with the Rabi frequency of the driving field and the slow time-dependent variations associated with a SF pulse. This procedure is very similar to a slowly varying amplitude and phase approximation, where fast oscillations with the optical frequency are separated from the slow time-dependent evolution of atomic variables and fields. So, finally a SF pulse shows up as an envelope filled by fast sinusoidal oscillations; see Fig. 2. The envelope is a solution of the reduced system of the Maxwell-Bloch equations, and the oscillations have a period equal to the inverse Rabi frequency of the driving field.

II. DESCRIPTION OF THE MODEL

Dicke has pointed out that there is nothing inherently quantum mechanical about superfluorescence, and a collection of classical dipoles appropriately prepared can exhibit

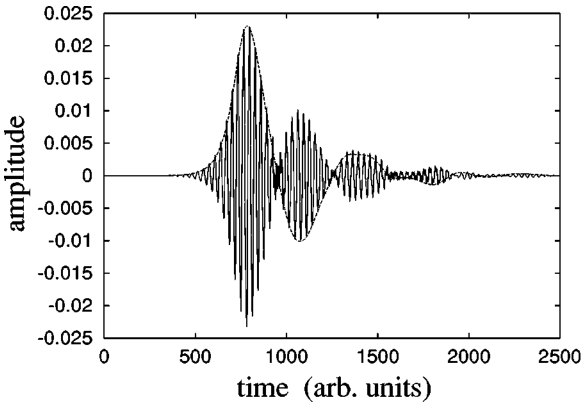

FIG. 2. Time dependence of the dimensionless field amplitude (normalized to the amplitude of the driving field Ω_0) at the rare end of the medium, $z=L$. Comparison of the exact numerical solution of Eqs. (1)–(9) with initial and boundary conditions (15) (solid line), and numerical solution of the equivalent system of Maxwell-Bloch equations (59)–(61) (dashed line). The parameters are $\rho_{ab}^0=10^{-7}$, $\Omega_0=\Omega_c$, $\rho_{aa}^0=0.2$, $\rho_{bb}^0=0.8$, and $\rho_{cc}^0=0$ for the three-level model; $\rho_{ab}^0=\frac{1}{30}\times 10^{-7}$, $\mathcal{N}^0=0.1$ for two-level model. Throughout all the numerics we put σ_{cb} and σ_{ab} equal to zero.

superfluorescent behavior; see Refs. [2] and [10]. Later, it has been shown in Refs. [11] and [12] that a simple theoretical model based on a semiclassical approach (classical fields, quantized atoms) accurately describes the features of the emitted radiation both in a mean-field approach and in a long (or dense) medium [11–13]. So, in our theoretical model the semiclassical approach is adopted, in order to take propagation effects fully into account [14].

Consider a V-type three-level system with the ground state $|b\rangle$ and excited states $|a\rangle$ and $|c\rangle$ as shown in Fig. 1. Transition $|b\rangle \leftrightarrow |c\rangle$ is driven by a strong field with Rabi frequency $\Omega(z,t)$. A probe pulse $\alpha(z,t)$ appears on the transition $|b\rangle \leftrightarrow |a\rangle$, resulting from the initial fluctuation in polarization ρ_{ab}. In the slowly varying envelope approximation, the temporal and spatial evolution of the fields are governed by the wave equations

$$\left(c\frac{\partial}{\partial z}+2\pi\sigma_{cb}\right)\Omega(z,t)=i\frac{\omega_{cb}\mu_{cb}^2 N}{\epsilon_0\hbar}\rho_{cb}, \tag{1}$$

$$\left(c\frac{\partial}{\partial z}+2\pi\sigma_{ab}\right)\alpha(z,t)=i\frac{\omega_{ab}\mu_{ab}^2 N}{\epsilon_0\hbar}\rho_{ab}, \tag{2}$$

where z is the propagation distance, and the real time t' is changed to the retarded time t: $t=t'-z/c$. ρ_{ab} and ρ_{cb} are off-diagonal density-matrix elements in the rotating frame, ω_{cb} and ω_{ab} are optical frequencies of the corresponding transitions, μ_{cb} and μ_{ab} are dipole matrix elements of the transitions $|c\rangle \leftrightarrow |b\rangle$ and $|a\rangle \leftrightarrow |b\rangle$ (supposed to be real, for simplicity), N is the density of atoms, and σ_{ab} and σ_{cb} account for the losses (including diffraction losses) of the fields inside a sample. Refractive indices on both transitions are chosen the same and put equal to unity. Slowly varying amplitudes of the driving and probe electric fields, E_Ω and E_α, are related to the Rabi frequencies Ω and α according to

$$E_\Omega=2\frac{\hbar\Omega}{\mu_{cb}},\quad E_\alpha=2\frac{\hbar\alpha}{\mu_{ab}}. \tag{3}$$

In our consideration we suppose the medium to be homogeneously broadened. The semiclassical density-matrix equations of motion under the rotating-wave approximation can be written as

$$\frac{\partial}{\partial t}\rho_{ab}=-\gamma_{ab}\rho_{ab}-i\alpha(\rho_{aa}-\rho_{bb})-i\Omega\rho_{ac}, \tag{4}$$

$$\frac{\partial}{\partial t}\rho_{ac}=-\gamma_{ac}\rho_{ac}+i\alpha\rho_{bc}-i\Omega^*\rho_{ab}, \tag{5}$$

$$\frac{\partial}{\partial t}\rho_{cb}=-\gamma_{cb}\rho_{cb}-i\Omega(\rho_{cc}-\rho_{bb})-i\alpha\rho_{ca}, \tag{6}$$

$$\frac{\partial}{\partial t}\rho_{aa}=-\gamma_a\rho_{aa}+r_a\rho_{bb}-i(\alpha^*\rho_{ab}-\alpha\rho_{ba}), \tag{7}$$

$$\frac{\partial}{\partial t}\rho_{bb}=\gamma_a\rho_{aa}+\gamma_c\rho_{cc}-(r_a+r_c)\rho_{bb}+i(\alpha^*\rho_{ab}-\alpha\rho_{ba})+i(\Omega^*\rho_{cb}-\Omega\rho_{bc}), \tag{8}$$

$$\frac{\partial}{\partial t}\rho_{cc}=-\gamma_c\rho_{cc}+r_c\rho_{bb}-i(\Omega^*\rho_{cb}-\Omega\rho_{bc}), \tag{9}$$

where γ_{ab}, γ_{ac}, and γ_{cb} are dephasing rates of polarizations; γ_a, γ_c, r_c, and r_a are the decay and pumping rates indicated in Fig. 1,

$$\gamma_{ab}=\frac{\gamma_a+r_a+r_c}{2}+\gamma_{ab}^{ph}, \tag{10}$$

$$\gamma_{ac}=\frac{\gamma_a+\gamma_c}{2}+\gamma_{ac}^{ph}, \tag{11}$$

$$\gamma_{cb}=\frac{r_a+r_c+\gamma_c}{2}+\gamma_{cb}^{ph}. \tag{12}$$

The last terms in Eqs. (10)–(12) correspond to the random perturbations of the levels, which lead to the phase damping of atomic states, while keeping the populations unchanged. Usually, such kinds of perturbations are induced by collisions in dense gaseous media, or by interaction with phonons in solids.

The analysis is referred to the case of the closed V-type system, so that one of the equations [Eqs. (7)–(9)] is to be replaced by the normalization condition

$$\rho_{aa}+\rho_{bb}+\rho_{cc}=1. \tag{13}$$

We assume, that the NV three-level atoms are confined into the active volume V, which has the shape of a cylinder with length L and cross-section area S ($L \gg \sqrt{S}$). Before the arrival of the driving pulse, $t'<0$, the medium is under the effect of continuous (or pulsed) incoherent pumping, and thereby is prepared in the following manner:

$$\rho_{bb}^0 \equiv \rho_{bb}(t<0) = \frac{1}{1+r_a/\gamma_a+r_c/\gamma_c},$$

$$\rho_{aa}^0 \equiv \rho_{aa}(t<0) = \frac{r_a/\gamma_a}{1+r_a/\gamma_a+r_c/\gamma_c}, \tag{14}$$

$$\rho_{cc}^0 \equiv \rho_{cc}(t<0) = \frac{r_c/\gamma_c}{1+r_a/\gamma_a+r_c/\gamma_c},$$

so that the initial state is incoherent; i.e., there are no correlations between the wave functions of the different atoms. At the moment $t'=0$ the pumping process is switched off, $r_a(t'\geqslant 0)=0$ and $r_c(t'\geqslant 0)=0$, and the atoms evolve independently in radiative decay.

The following initial and boundary conditions are used for the fields and polarizations:

$$\Omega(z,t'=0) = \begin{cases} \Omega_0, & z=0, \\ 0, & 0<z<L, \end{cases}$$

$$\Omega(z=0,t') = \begin{cases} 0, & t<0, \\ \Omega_0, & t\geqslant 0, \end{cases}$$

$$\alpha(z=0,t')=0,$$

$$\alpha(z,t'=0)=0, \tag{15}$$

$$\rho_{cb}(z,t'=0)=0,$$

$$\rho_{ac}(z,t'=0)=0,$$

$$\rho_{ab}(z,t'=0)=\rho_{ab}^0.$$

We will consider the case where initially there is no population inversion between the bare states $|a\rangle$ and $|b\rangle$ on the probe transition: $\rho_{aa}^0<\rho_{bb}^0$. If, in addition to that, there is an inversion on a two-photon transition $|a\rangle \rightarrow |b\rangle \rightarrow |c\rangle$, i.e., $\rho_{aa}^0>\rho_{cc}^0$, we say that the system is prepared in a state with Raman inversion. In the opposite case of $\rho_{aa}^0<\rho_{cc}^0$ there is no inversion of any kind.

Semiclassical density-matrix equations inherently do not contain any mechanism for spontaneous emission, so that an initially inverted system cannot evolve. This problem can be overcome by adding a phenomenological initial polarization ρ_{ab}^0 to simulate the effect of spontaneous emission. This term can be constructed to be consistent with the requirements of thermal equilibrium as well as energy and number conservation; see the paper by MacGillivray and Feld [12].

Three basic assumptions are incorporated into Eqs. (1)–(9): (i) the semiclassical model with an artificially introduced small initial polarization ρ_{ab}^0 to simulate spontaneous emission is used, instead of a quantized field model; (ii) the plane-wave approximation is utilized, thus effects associated with finite beam diameter are neglected, which is the good approximation for Fresnel numbers, $2S/\lambda L$, larger than 0.1 [15]; (iii) the interaction of forward and backward traveling waves is ignored.

Numerical solutions of Eqs. (1) and (2) and (4)–(9) will be presented in the following; however, approximate analytical solutions that are in a close agreement with the computer results will also be obtained in certain limiting cases. These results are useful as an aid to understanding the underlying physical processes.

III. REDUCED EQUATIONS

The effective self-induction of correlations between the atomic dipole moments of a two-level system can be possible only in a case where the evolution time T_R of the process is shorter than the phase relaxation time γ_{ab}^{-1} and also shorter than γ_a^{-1}. The same is certain to be applied for the $|a\rangle \leftrightarrow |b\rangle$ subsystem in the three-level configuration, such that a SF pulse has to be shorter than γ_a and γ_{ab}. It is a more complicated problem to realize intuitively a role for other relaxation rates, namely, γ_c, γ_{cb}, and γ_{ac}. It is known that a cw gain without inversion implies fast decay at the driving transition [1]. On the other hand, this relaxation may destroy the phase correlations between dipoles responsible for the SF process. A detailed discussion based on the numerical calculations is reserved for the succeeding sections. We give here only the general conclusion: the increasing in *any* decay rate results in the termination of the radiation process.

Thus, as for a two-level consideration, we keep the basic properties of a SF pulse unchanged in the limit when all γ's go to zero. In the lossless approximation

$$T_D,\, T_R,\, \alpha^{-1} \ll \text{all decay times}, \tag{16}$$

where T_D is the delay time, an analysis of the cumbersome system of equations (1)–(2) and (4)–(9) becomes simpler. In this section we show how the original system of density-matrix equations (4)–(9) can be reduced to the Bloch-type equations for a two-level system in the limit of sufficiently large intensities of the driving field, so that Ω^{-1} appears as the fastest characteristic time of the system,

$$\Omega^{-1} \ll T_R,\, \alpha^{-1}. \tag{17}$$

The fact that the final equations have the form of Bloch equations makes further consideration unnecessary, since the solutions of the form of SF pulses are well-known; see Refs. [14] and [16]. Some numericals, which are useful for going beyond the approximations and for comparison with the analytics, will be presented in Sec. IV.

At the initial moment, $t=0$, the driving field enters the medium exciting the polarization on the $|c\rangle \leftrightarrow |b\rangle$ transition, which leads in turn to the oscillation behavior of the population difference between these levels. Passing a medium in a time $t=L/c$, the field initiates the oscillations along the whole length L of a sample. We choose the length to be short enough, so that influence of these oscillations back on the field is negligible,

$$L \ll \Omega_0 \frac{\epsilon_0 \hbar c}{\omega_{cb}\mu_{cb}^2 N}, \tag{18}$$

and Rabi frequency may be considered as a constant value throughout the sample. We also assume that

$$\frac{L}{c} \ll T_R,\, T_D. \tag{19}$$

The inequality (19) implies that the photons of the probe field leave the active volume in a time that is shorter than the characteristic time of evolution of the interatomic correlations; hence, the stimulated processes on the $|a\rangle \leftrightarrow |b\rangle$ transition are unimportant during the emission.

The formal solution for the evolution of the $|c\rangle - |b\rangle$ subsystem can be found from Eqs. (6), (7), and (9),

$$(\rho_{cc}-\rho_{bb}) = n_{cb}^0 \cos(2\Omega_0 t) - \frac{\alpha}{\Omega_0}\rho_{ca} + \int_0^t \frac{\partial}{\partial t'}\left[\rho_{aa}+\frac{\alpha}{\Omega_0}\rho_{ca}\right]\cos[2\Omega_0(t'-t)]dt', \tag{20}$$

$$\rho_{cb} = -\frac{i}{2} n_{cb}^0 \sin(2\Omega_0 t) + \frac{i}{2}\int_0^t \frac{\partial}{\partial t'} \times \left[\rho_{aa}+\frac{\alpha}{\Omega_0}\rho_{ca}\right]\sin[2\Omega_0(t'-t)]dt', \tag{21}$$

with

$$n_{cb}^0 = \rho_{cc}^0 - \rho_{bb}^0. \tag{22}$$

The first terms in the left-hand side of solutions (20) and (21) describe the well-known Rabi oscillations between the two levels. If the probe field appearing on the adjacent transition $|a\rangle \leftrightarrow |b\rangle$ does not reach an appreciable value, such that $\alpha \ll \Omega_0$ takes place, the contribution of higher harmonics to the dynamics on the $|c\rangle \leftrightarrow |b\rangle$ transition vanishes. The same inequality allows us to neglect the second term in Eq. (20). However, we should take into account the *dc* component as well as those parts of integrals in Eqs. (20) and (21) that oscillate with frequency $2\Omega_0$. Let us introduce the Fourier components $\overline{f}$, f_c, and f_s in the following way:

$$\frac{\partial}{\partial t}\left[\rho_{aa}+\frac{\alpha}{\Omega_0}\rho_{ca}\right] = \frac{\partial \overline{f}}{\partial t} + 2\frac{\partial f_c}{\partial t}\cos(2\Omega_0 t) + 2\frac{\partial f_s}{\partial t}\sin(2\Omega_0 t), \tag{23}$$

where we have neglected all the higher harmonics. $\overline{f}$, f_c, and f_s are supposed to vary slowly compared to Ω_0^{-1}. At the end of our calculations we find the relationships between the Fourier components and real atomic and field variables.

Now we can rewrite Eqs. (20) and (21) in a shorter form,

$$\rho_{cc}-\rho_{bb} = (n_{cb}^0 + f_c)\cos(2\Omega_0 t) - f_s \sin(2\Omega_0 t), \tag{24}$$

$$\rho_{cb} = -\frac{i}{2}(n_{cb}^0 + f_c)\sin(2\Omega_0 t) - \frac{i}{2} f_s \cos(2\Omega_0 t). \tag{25}$$

Using Eq. (24) and the conservation law of the form of Eq. (13), we express the population of the $|b\rangle$ state in terms of ρ_{aa} and the Fourier components, f_s and f_c,

$$\rho_{bb} = \frac{1}{2}[1-\rho_{aa} + f_s \sin(2\Omega_0 t) - (n_{cb}^0 + f_c)\cos(2\Omega_0 t)]. \tag{26}$$

Finally the density-matrix equations for the polarizations reduce to

$$\frac{\partial}{\partial t}\rho_{ab} = -i\Omega_0 \rho_{ac} - \frac{i}{2}\alpha[3\rho_{aa} - 1 - f_s \sin(2\Omega_0 t) + (n_{cb}^0 + f_c)\cos(2\Omega_0 t)], \tag{27}$$

$$\frac{\partial}{\partial t}\rho_{ac} = -i\Omega_0 \rho_{ab} - \frac{1}{2}\alpha[f_s \cos(2\Omega_0 t) + (n_{cb}^0 + f_c)\sin(2\Omega_0 t)]. \tag{28}$$

Polarization ρ_{ab} and two-photon coherence ρ_{ac} appear in Eqs. (27) and (28) symmetrically, and we can easily decouple the equations in terms of the new variables,

$$R = \rho_{ab} + \rho_{ac}, \quad Q = \rho_{ab} - \rho_{ac}.$$

Now the equations for R and Q become

$$\frac{\partial}{\partial t}R = -i\Omega_0 R - \frac{i}{2}\alpha[3\rho_{aa} - 1 + n_{cb}^0 + f_c - i f_s] \times \exp(-2i\Omega_0 t), \tag{29}$$

$$\frac{\partial}{\partial t}Q = i\Omega_0 Q - \frac{i}{2}\alpha[3\rho_{aa} - 1 + n_{cb}^0 + f_c + i f_s]\exp(+2i\Omega_0 t). \tag{30}$$

Then the formal solution for R and Q reads

$$R = -\frac{i}{2}\int_0^t \alpha\{(3\rho_{aa}-1)\exp[+i\Omega_0(t'-t)] + [n_{cb}^0 + f_c - i f_s]\exp[-i\Omega_0(t'+t)]\}dt', \tag{31}$$

$$Q = -\frac{i}{2}\int_0^t \alpha\{(3\rho_{aa}-1)\exp[-i\Omega_0(t'-t)] + [n_{cb}^0 + f_c + i f_s]\exp[+i\Omega_0(t'+t)]\}dt'. \tag{32}$$

Now using the definitions for R and Q and the solutions (31) and (32), one can find the explicit solutions for the off-diagonal density-matrix elements ρ_{ab} and ρ_{ac},

$$\rho_{ab} = -\frac{i}{2}\int_0^t \alpha\{(3\rho_{aa}-1)\cos[\Omega_0(t'-t)] + (n_{cb}^0 + f_c)\cos[\Omega_0(t'+t)] - f_s \sin[\Omega_0(t'+t)]\}dt', \tag{33}$$

$$\rho_{ac} = \frac{1}{2}\int_0^t \alpha\{(3\rho_{aa}-1)\sin[\Omega_0(t'-t)] - (n_{cb}^0 + f_c) \times \sin[\Omega_0(t'+t)] + f_s \cos[\Omega_0(t'+t)]\}dt'. \tag{34}$$

It is seen from Eqs. (33) and (34) that both polarizations contain two quadrature components oscillating rapidly with frequency Ω_0. The same modulation is superimposed on the probe field α through the propagation equation (2). Separating this fast motion one can represent the polarizations ρ_{ab}

and ρ_{ac}, as well as the field α, in terms of envelope functions according to the following definitions:

$$\rho_{ab}=r^s_{ab}\sin(\Omega_0 t)+r^c_{ab}\cos(\Omega_0 t), \tag{35}$$

$$\rho_{ac}=r^s_{ac}\sin(\Omega_0 t)+r^c_{ac}\cos(\Omega_0 t), \tag{36}$$

$$\alpha=\alpha_s\sin(\Omega_0 t)+\alpha_c\cos(\Omega_0 t). \tag{37}$$

This procedure is very similar to the separation of fast terms in the slowly varying amplitude and phase approximation. And referring to the latter we neglect the contribution of the terms oscillating with higher frequencies, which are of the order of α/Ω and less. In such a manner one usually keeps only the *dc* component of the population difference while considering two-level atoms. However, this is not the case here, where two-photon processes play an important role. Thus, for the self-consistent description of the three-level system we should keep the *dc* component of ρ_{aa} along with sine and cosine ones,

$$\rho_{aa}=\overline{n}+n_s\sin(2\Omega_0 t)+n_c\cos(2\Omega_0 t). \tag{38}$$

Formally, the reason for keeping the oscillating terms in Eq. (38) is clearly seen from the solutions (20) and (21). A couple of steps further we find that n_s and n_c are of the order of α/Ω_0. However, they cannot be neglected, because the integrals in Eqs. (20) and (21) contain the derivatives of ρ_{aa}, which give an additional factor of Ω_0 after differentiation. The same reason is valid for keeping the ρ_{ca} terms in the integrals.

After substitution of expansions (35), (36), and (37) into (33) and (34) with the subsequent separation of fast terms, we come to the simple equations for the envelope functions,

$$\frac{\partial}{\partial t}r^c_{ab}=-\frac{i}{4}[3\overline{n}-1+n^0_{cb}+f_c]\alpha_c+\frac{i}{2}f_s\alpha_s, \tag{39}$$

$$\frac{\partial}{\partial t}r^s_{ab}=-\frac{i}{4}[3\overline{n}-1-n^0_{cb}-f_c]\alpha_s+\frac{i}{2}f_s\alpha_c, \tag{40}$$

$$\frac{\partial}{\partial t}r^c_{ac}=+\frac{1}{4}[3\overline{n}-1-n^0_{cb}-f_c]\alpha_s+\frac{1}{2}f_s\alpha_c, \tag{41}$$

$$\frac{\partial}{\partial t}r^s_{ac}=-\frac{1}{4}[3\overline{n}-1+n^0_{cb}+f_c]\alpha_c-\frac{1}{2}f_s\alpha_s, \tag{42}$$

$$\frac{\partial}{\partial t}\overline{n}=-i(\alpha_s r^s_{ab}+\alpha_c r^c_{ab}), \tag{43}$$

$$2\Omega_0 n_c=i(\alpha_c r^s_{ab}+\alpha_s r^c_{ab}), \tag{44}$$

$$2\Omega_0 n_s=i(\alpha_s r^s_{ab}-\alpha_c r^c_{ab}). \tag{45}$$

Coming back to the definitions for the Fourier coefficients $\overline{f}$, f_s, and f_c, see Eq. (23), we now can express them in terms of the envelope functions,

$$\overline{f}=\overline{n}-\overline{n}|_{t=0}, \tag{46}$$

$$f_c=\Omega_0\int_0^t n_s\,dt'+\frac{1}{2}\int_0^t(\alpha_s r^c_{ca}+\alpha_c r^s_{ca})\,dt', \tag{47}$$

$$f_s=\Omega_0\int_0^t n_c\,dt'+\frac{1}{2}\int_0^t(\alpha_s r^s_{ca}-\alpha_c r^c_{ca})\,dt'. \tag{48}$$

Equations (39)–(45) for slowly varying quadrature components of ρ_{ab}, ρ_{ac}, ρ_{aa}, and α describe the whole class of coherent phenomena taking place in a three-level system driven by a strong cw field. They seem rather complicated because the sine and cosine components (α_s and α_c) of the probe field turn out to be coupled through the atomic variables. However, we do not need to solve the system of equations in the general form (39)–(45) in order to describe the SF phenomenon. In the following we show that only one quadrature component survives in a medium with no population inversion between states $|a\rangle$ and $|b\rangle$.

IV. MAXWELL-BLOCH EQUATIONS

Let us consider the initial stage of evolution of a SF pulse, when the field is weak enough, so that the linear approximation on α_c and α_s is applicable. Equations (39)–(45) become uncoupled in this limit and we get only two differential equations for the components of polarization,

$$\frac{\partial}{\partial t}r^c_{ab}=-\frac{i}{2}[\rho^0_{aa}-\rho^0_{bb}]\alpha_c, \tag{49}$$

$$\frac{\partial}{\partial t}r^s_{ab}=-\frac{i}{2}[\rho^0_{aa}-\rho^0_{cc}]\alpha_s, \tag{50}$$

and the correspondent components of the two-photon coherence follow the polarization with a $\pi/2$ shift,

$$r^s_{ac}=-i\,r^c_{ab}, \tag{51}$$

$$r^c_{ac}=+i\,r^s_{ab}. \tag{52}$$

The SF effect originally starts from a weak spontaneous emission, and the generated SF pulse contains only those frequency components of the field that experienced gain on a linear stage of evolution. The initial inversionless condition $\rho^0_{aa}<\rho^0_{bb}$ results in an absorption of the cosine component of the field. So, even though the spontaneous emission contributes to α_c, this mode will eventually decay. On the other hand, if the system is prepared in a state with initial Raman inversion, $\rho^0_{aa}>\rho^0_{cc}$, the α_s component will experience gain. So, we conclude that the SF pulse evolves only in the system with initial Raman inversion and contains only one mode of radiation, namely, α_s.

Coming back to the full system of equations (39)–(45) and putting α_c equal to zero, we have for the Fourier components,

$$\overline{f}=\overline{n}-\overline{n}|_{t=0}, \tag{53}$$

$$f_c=\overline{n}|_{t=0}-\overline{n}, \tag{54}$$

$$f_s=0, \tag{55}$$

and for the components of the population of $|a\rangle$ state,

$$\frac{\partial}{\partial t}\overline{n} = -i\,\alpha_s\,r^s_{ab}, \tag{56}$$

$$n_c = 0, \tag{57}$$

$$2\Omega_0\,n_s = +i\,\alpha_s\,r^s_{ab}. \tag{58}$$

Finally we get for the SF field a self-consistent system of equations of the Maxwell-Bloch type:

$$\left(c\frac{\partial}{\partial z} + 2\pi\sigma_{ab}\right)\mathcal{E}(z,t) = i\,\Omega_c^2\,\mathcal{P}, \tag{59}$$

$$\frac{\partial}{\partial t}\mathcal{P} = -i\,\mathcal{N}\mathcal{E}, \tag{60}$$

$$\frac{\partial}{\partial t}\mathcal{N} = -2i(\mathcal{E}^*\mathcal{P} - \mathcal{E}\mathcal{P}^*), \tag{61}$$

with the following definitions of inversion, polarization, and field,

$$\mathcal{N} = \frac{2\overline{n} - \rho^0_{aa} - \rho^0_{cc}}{2}, \tag{62}$$

$$\mathcal{P} = \frac{r^s_{ab}}{2}, \tag{63}$$

$$\mathcal{E} = \frac{\alpha_s}{2}. \tag{64}$$

In Eq. (59) we introduced the cooperative frequency Ω_c,

$$\Omega_c = \sqrt{\frac{\omega_{ab}\mu^2_{ab}N}{\epsilon_0\hbar}}. \tag{65}$$

The closed system of equations (59)–(61) constitutes the main analytical result of the paper, demonstrating that the envelope of a SF pulse evolves in a three-level medium driven by a strong coherent cw field as if it were a two-level medium with the initial population difference

$$\mathcal{N}^0 = \frac{\rho^0_{aa} - \rho^0_{cc}}{2}. \tag{66}$$

The sine component of the probe field experiences gain with an increment that is proportional to the Raman population inversion $\Omega_c^2\,\mathcal{N}_0$, contrary to a two-level system, where the increment depends on the population difference between lower and upper states. Let us stress here that this is not a real increment for a weak field, because we initially have set at zero the decaying components of polarization, r^c_{ab} and r^s_{ac}. A more accurate study of a linear regime has to include the interplay between sine and cosine modes.

The developed Maxwell-Bloch formalism gives an additional advantage in understanding the SF phenomenon in the driven three-level system. Thus, all the properties of the two-level SF can be simply transferred to the three-level configuration.

V. EVOLUTION ON THE DRIVING TRANSITION

Now, having the explicit expressions for the Fourier components of the form of Eqs. (53)–(55), one can describe the evolution of atomic variables in the driving transition. Substituting Eqs. (54) and (55) into Eqs. (24)–(26), we get

$$\rho_{bb} = (\mathcal{N}^0 + \rho^0_{cc} - \mathcal{N}) + (1 + \mathcal{N} - 3\rho^0_{cc} - 3\mathcal{N}^0)\cos^2(\Omega_0 t), \tag{67}$$

$$\rho_{cc} = (\mathcal{N}^0 + \rho^0_{cc} - \mathcal{N}) + (1 + \mathcal{N} - 3\rho^0_{cc} - 3\mathcal{N}^0)\sin^2(\Omega_0 t), \tag{68}$$

$$\rho_{cb} = \frac{i}{2}(1 + \mathcal{N} - 3\rho^0_{cc} - 3\mathcal{N}^0)\sin(2\Omega_0 t). \tag{69}$$

As long as the probe field does not considerably change the population of the $|a\rangle$ state, i.e., $\mathcal{N} \approx \mathcal{N}^0$, the driving transition experiences familiar Rabi oscillations near the equilibrium value $[(1-\rho^0_{aa})/2]$ with an amplitude equal to $1-\rho^0_{aa} - 2\rho^0_{cc}$. Increasing the probe field is accompanied by removing the population from the $|a\rangle$ state. Once all the excited atoms have transferred their energy to the probe field, i.e., inversion $\mathcal{N}$ has changed sign, $\mathcal{N} \to -\mathcal{N}^0$, the SF process is completed. The Rabi oscillations still take place between the $|b\rangle$ and $|c\rangle$ states, but with a reduced amplitude $(1-2\rho^0_{aa} - \rho^0_{cc})$ and an increased equilibrium value $[(1-\rho^0_{cc})/2]$.

As followed from Eqs. (41) and (42), the sine component of the two-photon coherence vanishes as a result of the suppression of the α_c mode. The cosine component behaves identically to the polarization $\mathcal{P}$, possessing additionally a constant $\pi/2$ phase shift

$$\frac{\partial}{\partial t}r^c_{ac} = 2\,\mathcal{N}\mathcal{E}. \tag{70}$$

The linear amplitude losses σ_{cb} have no effect on our analytics as long as condition (17) takes place. If $\sigma_{cb} \neq 0$, one simply needs to change the constant value Ω_0 everywhere to a new space-dependent variable

$$\Omega_0 \to \Omega_0 \exp\left[-\frac{2\pi\sigma_{cb}}{c}z\right]. \tag{71}$$

VI. NUMERICAL SIMULATIONS

Numerical simulations have been performed to prove the analytical speculations and to supplement them, going beyond the majority of the approximations made above. Figure 3 shows the typical shape of the SF pulse [see curve (1)] in the driven system obtained from the exact numerical calculations of the full set of Eqs. (1), (2), and (4)–(9) with initial and boundary conditions given by Eqs. (14) and (15). The pulse displays the characteristic oscillatory behavior according to the above analytical predictions; see Eq. (37). Moreover, under our hypothesis, the slowly varying envelope of curve (1) has to be fitted by the solution of the reduced (Maxwell-Bloch) system of equations, (59)–(61). Indeed, curve (2) perfectly fits all the lobes of radiation. However, it is worth pointing out that for such a good agreement we would have to use two different numerical values for the initial spontaneous polarization ρ^0_{ab}.

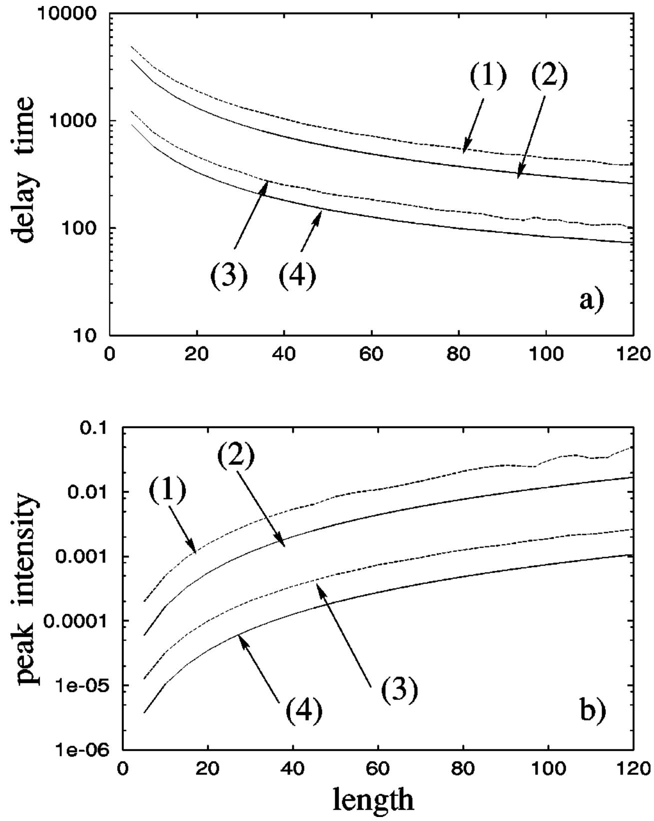

FIG. 3. (a) Delay time (arb. units) and (b) dimensionless peak intensity (normalized to Ω_0^2) of the first burst of radiation versus the length of a sample (arb. units). For three-level numericals [curves (1) and (3)] the parameters are $\rho_{ab}^0=10^{-7}$, $\rho_{aa}^0=0.2$, $\rho_{bb}^0=0.8$, and $\rho_{cc}^0=0$. For two-level numericals [curves (2) and (4)] the parameters are $\rho_{ab}^0=10^{-7}$, $\mathcal{N}^0=0.1$. $\Omega_0=\Omega_c$ for curves (1) and (2); the cooperative frequency for curves (3) and (4) is 4 times smaller without changes in the value of Ω_0.

The numerical simulations that have been performed with the same value of initial polarization ρ_{ab}^0 show that the delay time for the two-level problem is always shorter than for the full three-level analysis; see Fig. 3(a). At least two different reasons can be given to explain the inconsistency. First, it is a direct consequence of the difference between the boundary conditions for the two problems. The analytical derivation essentially utilizes the requirement that the Rabi oscillations on the driving transition be already established throughout a sample. It is equivalent to the uniformly excited (the entire system inverted simultaneously) two-level system, and the radiation grows throughout the sample from the same level of initial fluctuations, namely, ρ_{ab}^0. On the other hand, the real three-level system is prepared with no population inversion between the bare states $|a\rangle$ and $|b\rangle$, and therefore absorbs the radiation energy in the absence of the driving field. It starts to emit only after the arrival of the drive pulse, so that the atoms at the rare end of the sample absorb the radiation during the escape time, $t=L/c$, and appear to be involved in the coherent evolution only for $t>L/c$. This is very similar to swept excitation (system inverted by a pulse traveling longitudinally through the medium at the speed of light) of a two-level system [17]. So, the difference in the starting conditions for the SF pulse for the two approaches can differ significantly.

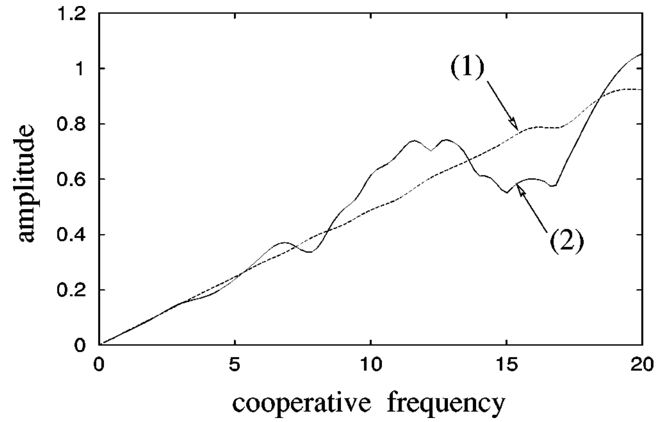

FIG. 4. Dependence of the absolute value of a dimensionless peak amplitude on the cooperative frequency for (1) the two-level configuration; (2) the three-level configuration. The amplitude and cooperative frequency are plotted in units of Rabi frequency Ω_0.

The second reason is also the consequence of the simplification accepted in the reduced equations. We have mentioned earlier that the two-level model cannot fully describe the linear stage of evolution of the SF field, since the decaying components of polarization and two-photon coherence were put to zero. Their influence might be important at the very start of evolution of the SF pulse.

The above arguments are only of a qualitative type and should be treated as a partial explanation for the observed distinction in the delay times. Note here that further discussion on the choice of a certain value of ρ_{ab}^0 is of doubtful benefit in the framework of the semiclassical approach, where this parameter is included phenomenologically. So, we leave the detailed consideration of the initial stage of SF evolution to further quantum-mechanical treatments, in which the spontaneous-emission process can be described in a natural way.

It is a well-established fact that the longer the delay time, the shorter the pulses that are generated, and therefore the higher the amplitudes they have. Since the three-level medium exhibits longer delay compared to the two-level configuration, we should expect the generation of more intense pulses. Figure 3(b) lives up to our expectations, showing the length dependence of the intensity of the first burst of radiation. All the curves are similar and have the quadratic dependence of the peak intensity on the length, which can be thought of as a manifestation of the SF effect. Note here that, for the rather long samples, Fig. 3 displays small deviations from the smooth curve. This behavior becomes clear if we recall that the duration of a SF pulse decreases linearly with increasing length. So the number of oscillations covered by the envelope reduces progressively, and, hence, the position of the maximum associated with the oscillation peak becomes less undetermined.

Another, more direct verification of the SF effect is illustrated in Fig. 4, where the amplitude dependence on the atomic density (cooperative frequency) is displayed. The linear behavior of the curves for relatively small values of the cooperative frequency corresponds to the growth of peak intensity as N^2 and, thus, gives an indication of the SF effect. As long as the peak amplitude of the probe field is small enough (more than three times smaller for Fig. 4) compared

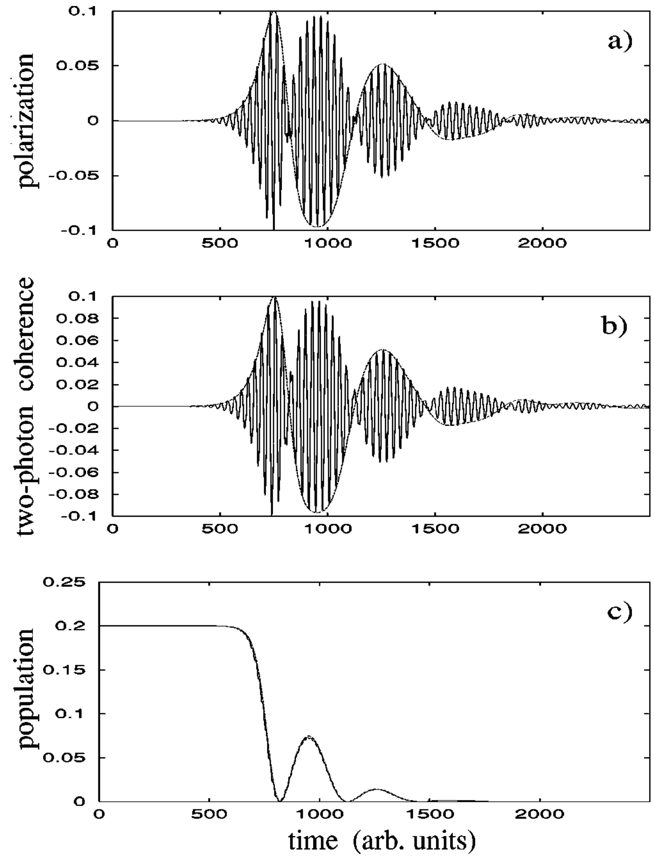

FIG. 5. Comparison of the exact numerical solution of Eqs. (1)–(9) with initial and boundary conditions (15) and the numerical solution of the equivalent system of Maxwell-Bloch equations (59)–(61): (a) polarization ρ_{ab} (solid line) and $\mathcal{P}$ (dashed line); (b) polarization ρ_{ac} (solid line) and $\mathcal{P}$ (dashed line); (c) population ρ_{aa} (solid line) and $(\mathcal{N}+\mathcal{N}^0)$ (dashed line), almost indistinguishable. All the curves are plotted for the point at the rare end of the medium, $z=L$. The parameters are the same as for Fig. 2.

to the driving field, the results for the two-level computation copy the output for the full three-level model. With a further increase in intensity the analytically predicted agreement becomes inapplicable, and the pulse shape (not shown) takes a chaotic structure without any visible regularities. In other words, the consideration in terms of fast oscillations modulated by a slowly varying envelope becomes incorrect. Two different effects come into play with the density growth: (i) the self-action of the probe pulse through the interaction with the coupling transition; and (ii) the effect of stimulated emission, i.e., the amplification of the pulse due to the propagation through an extremely dense sample. The latter is also responsible for deviations from the perfect line for the two-level configuration.

As we have mentioned in Sec. IV, only the sine components of ρ_{ab} and α can survive in the inversionless medium. In a similar spirit, the sine component of the two-photon coherence decays, while the cosine one, r^c_{ac}, displays exactly the same time-dependent behavior as r^s_{ab}; see Eq. (70). Figures 5(a) and 5(b) show the time evolution of the polarization ρ_{ab} and two-photon coherence ρ_{ac} for the atoms located at the rare end of the sample $(z=L)$. The envelopes are identical for both the curves and are obtained from the numericals on the two-level model (59)–(61) as a solution for

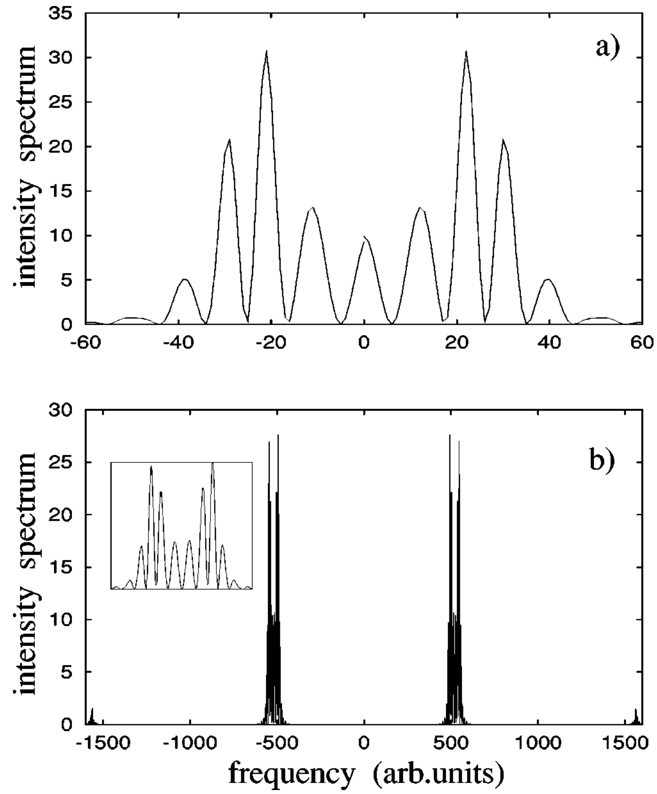

FIG. 6. Intensity spectra (arb. units) of the SF pulses, which are shown in Fig. 2. (a) Two-level model; (b) three-level model, inset shows the detailed structure of the left component centered at $\omega=-520$.

the polarization $\mathcal{P}$. One can see that $\mathcal{P}(t)$ faithfully copies the slowly varying variations of ρ_{ab} and ρ_{ac}. The temporal dynamics of the population of the $|a\rangle$ state, ρ_{aa}, is displayed in Fig. 5(c) by a solid line. As one could expect from analytical consideration, it changes slowly in time and does not exhibit any noticeable fast variations associated with Rabi oscillations on the coupling transition. Again, the numerical simulations perfectly match the two-level computations (dashed curve). Note here that variations in the Rabi frequency of the driving field do not affect the parameters of a SF pulse, and change only the density of oscillations under the pulse envelope.

The spectral characteristics of a SF pulse contain additional information about the underlying physics. Thus, Fig. 6(b) displays a spectrum of an output SF pulse with widely separated peaks, which are arranged symmetrically near the resonance frequency. Such a shape is a direct manifestation of the dynamic Stark splitting of the ground level under the action of a strong driving field applied on the coupling transition. The fine structure of each of the peaks reproduces all the features of a SF spectrum for a two-level medium; see Fig. 6(a). So, the separation of the fast and slow motions in the temporal representation is embodied in the spectral picture in the form of distant harmonics (as the result of fast oscillations), each displaying the internal structure (associated with the slowly varying envelope). A closer look at Fig. 6(b) allows us to detect the presence of harmonics oscillating with double frequency. It is precisely these terms that are neglected in our theoretical treatment.

So far, we have discussed primarily the temporal behavior

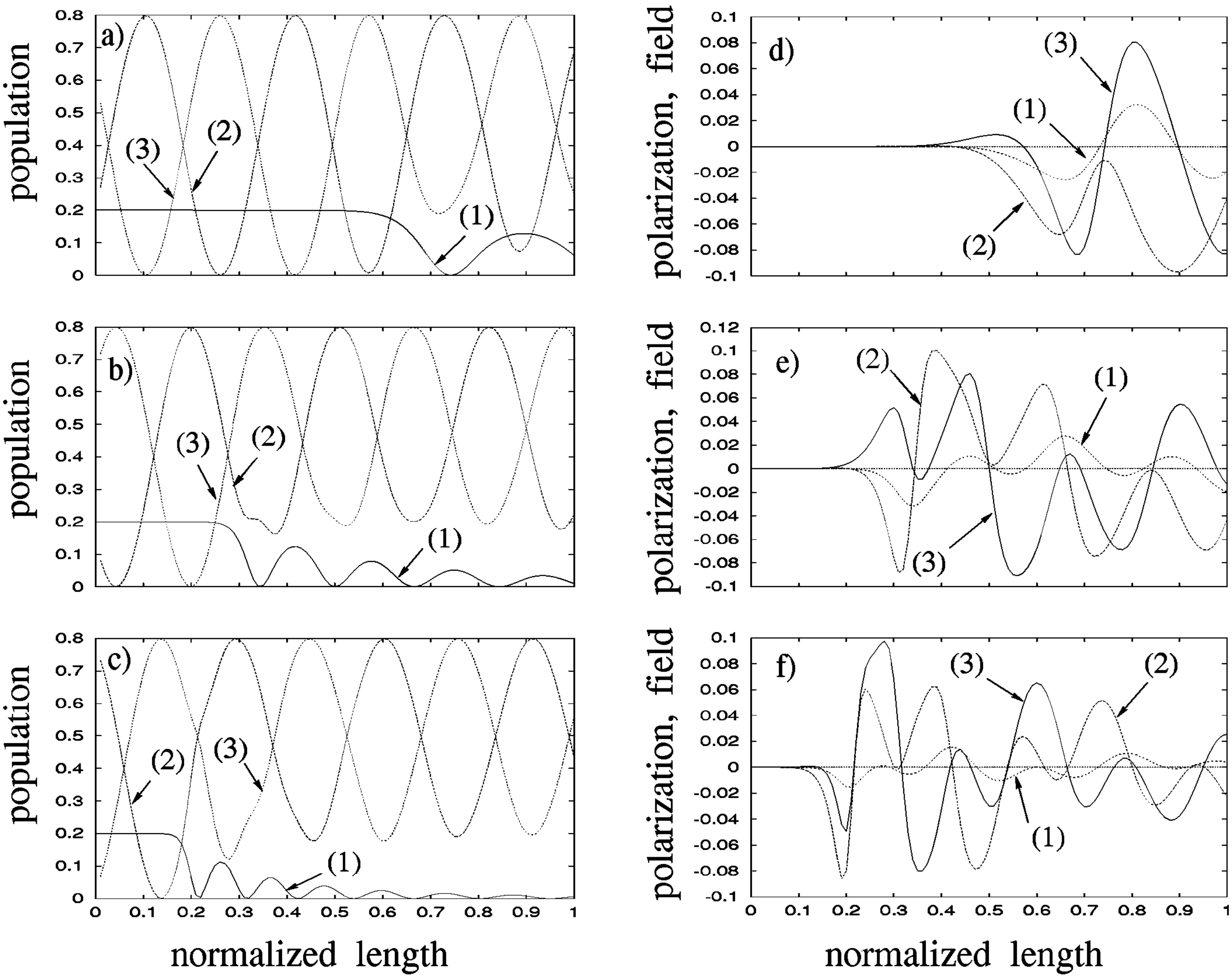

FIG. 7. Plots of the populations (1) ρ_{aa}, (2) ρ_{bb}, and (3) ρ_{cc} as functions of z/L (along the sample) at (a) $t=300$, (b) $t=600$, and (c) $t=900$. Plots of (1) the probe field α, (2) the polarization ρ_{ab}, and (3) the two-photon coherence ρ_{ac} as functions of z/L (along the sample) at (d) $t=300$, (e) $t=600$, and (f) $t=900$. The dimensionless field is normalized to Ω_0.

of field and atomic variables. To complete the analysis let us consider spatial propagation effects, which strongly influence the shape of a SF pulse in an extended SF system, as was fully realized in Ref. [12]. In the Bloch formalism for a point sample, a totally inverted system corresponds to a vector pointing straight up, analogous to a rigid pendulum balanced exactly on end. Similarly, the initially inverted extended medium corresponds to a spatial distribution of Bloch vectors all pointing straight up. However, as was pointed out in Ref. [12], the individual Bloch vectors of the extended medium, which are coupled together via the common radiation field, may evolve differently, owing to propagation effects. The regenerative amplification process leads to a rapid deexcitation of a certain region of the medium, after which essentially all of the population is brought into the lower level; i.e., the Bloch vectors all point downward. Deexcited regions can then be reexcited by the radiation from other regions, which gives rise to the ''ringing'' observed in the output radiation. As one can see from Fig. 7, a similar behavior is typical for the driven system as well. Additionally to the spatial evolution of the two components of the Bloch vector (here, ρ_{ab} and ρ_{aa}), the other elements of the three-level density matrix also display slow space variations. Thus, the nearly harmonic exchange of populations between $|b\rangle$ and $|c\rangle$ states is simply the space distribution of Rabi oscillations having the space-time dependence of the form of $(t'-z/c)$; see Eqs. (67) and (68).

Summarizing the numerical results, we conclude that the equivalent Maxwell-Bloch system of equations perfectly describes the basic features of the SF phenomenon in a three-level medium for large values of the driving field. There is no need for further consideration in the sense that the two-level SF is well studied, and all the results obtained in the previous works can simply be extended to the three-level configuration.

VII. DISCUSSION

Let us consider in detail the dynamics underlying the amplification process of the spontaneous field on the probe transition. We start from the linear stage of evolution, when the probe field is not of an appreciable value. Then, the populations on the driving transition oscillate between the $|b\rangle$ and $|c\rangle$ states with an amplitude equal to $\rho_{bb}^0-\rho_{cc}^0$, while ρ_{aa}

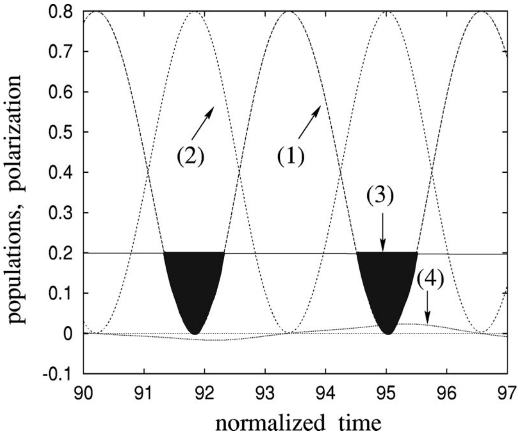

FIG. 8. Two periods of Rabi oscillations of populations on the driving transition, ρ_{bb} [curve (1)] and ρ_{cc} [curve (2)], for the point at the rare end of the medium, $z=L$. The temporal evolution of ρ_{aa} and ρ_{ab} is shown by curves (3) and (4), correspondingly. Time is in units of Ω_0^{-1}. The shaded regions indicate ''windows'' of bare inversion, i.e., when $\rho_{aa}>\rho_{bb}$.

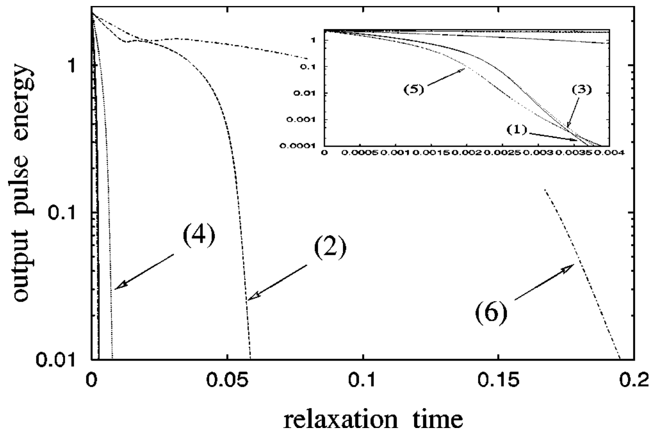

FIG. 9. Energy (arb. units) dependence of the SF pulse on the relaxation rates (1) γ_{ab} for $\gamma_a \gg \gamma_{ab}^{ph}, \gamma_{cb}^{ph}, \gamma_{ac}^{ph}, \gamma_c$; (2) γ_{ab} for $\gamma_{ab}^{ph}=\gamma_{ac}^{ph} \gg \gamma_a, \gamma_c, \gamma_{cb}^{ph}$; (3) γ_{cb} for $\gamma_c \gg \gamma_{ab}^{ph}, \gamma_{cb}^{ph}, \gamma_{ac}^{ph}, \gamma_a$; (4) γ_{cb} for $\gamma_{cb}^{ph}=\gamma_{ac}^{ph} \gg \gamma_a, \gamma_c, \gamma_{ab}^{ph}$; (5) γ_{ab} for $\gamma_a \gg \gamma_{ab}^{ph}$; (6) γ_{ab} for $\gamma_{ab}^{ph} \gg \gamma_a$. Curves (5) and (6) are plotted for the equivalent two-level system. Parameters for the three-level and two-level systems are the same as for Fig. 2. The inset shows the details that are not resolvable in the plot.

keeps its initial value ρ_{aa}^0; see Fig. 8. Similar oscillations take place in space, which is clearly seen in Figs. 7(a)–7(c). As we have shown previously, the SF develops only in a system with initial Raman inversion, such that state $|a\rangle$ is to be populated more than state $|c\rangle$ at $t=0$. This condition implies that the ''windows'' of bare inversion ($\rho_{aa}>\rho_{bb}$) and Raman inversion ($\rho_{aa}>\rho_{cc}$) are opened for a certain period of time. Looking at a period of Rabi oscillations one can see that the windows of bare inversion coincide with windows of Raman absorption, and vice versa. However, averaging the populations over a period of Rabi oscillations, and keeping in mind the inversionless condition $\rho_{aa}^0<\rho_{bb}^0$, we get

$$(\rho_{aa})_{av}<(\rho_{cc})_{av}\leqslant(\rho_{bb})_{av}, \tag{72}$$

i.e., the area of the absorption windows is larger than the area of the ''amplification windows.'' In spite of that, a probe radiation experiences gain, and the inequality (72) allows us to classify it as a ''LWI gain in average.''

The polarization ρ_{ab}, which oscillates with a doubled Rabi period, is zero exactly at the points of largest one-photon absorption (and largest Raman inversion, correspondingly); see Fig. 8. On the other hand, ρ_{ab} develops their nonzero (negative and positive) portions when windows of bare inversion are opened. Averaging over two periods of Rabi oscillations (corresponding to one period of ρ_{ab} oscillations) we finally get an amplification for the probe field, i.e., $(\rho_{ab})_{av}>0$.

The above consideration helps us to understand why one mode of radiation (its sine component) amplifies, while the other vanishes. The suppressed mode (cosine component) oscillates with a $\pi/2$ phase shift, such that the extrema of ρ_{ab} coincide with peaks of bare absorption, and hence, on average the probe field loses energy.

Based on our numerical calculations, showing that any relaxation process leads to the termination of the SF effect, we have neglected them completely through our analysis. After a discussion of the ideal SF is a proper place to take various decay channels into consideration, and to analyze the role of each decay constant.

The decay of ρ_{ab} plays the same role as that for a simple two-level system, resulting in the destruction of the cooperative behavior of atomic dipoles at the $|a\rangle \leftrightarrow |b\rangle$ transition. Curves (1) and (2) of Fig. 9 are plotted for a dilute (where $\gamma_{ab}^{ph} \ll \gamma_a$) and for a dense (where $\gamma_{ab}^{ph} \gg \gamma_a$) medium, respectively. One can see that the decay of population of state $|a\rangle$ has a much more dramatic effect on pulse energy than the pure dephasing processes, γ_{ab}^{ph}, which are not accompanied by changes in populations.

It is interesting to note that the decay rates of both upper levels, γ_a [see curve (1) in Fig. 9] and γ_c [see curve (3) in Fig. 9], produce an almost identical effect on pulse energy. This can be easily understood in terms of inversion windows. As we have learned from the above consideration, the amplification rate of a SF pulse is proportional to the areas of these windows. The decay of population from the $|a\rangle$ state continuously lowers the upper borders of the windows, resulting in a decrease of their total area. On the other hand, the decay from the $|c\rangle$ state gradually reduces the amplitude of the Rabi oscillations, while keeping their equilibrium value, $\rho_{bb}^0-\rho_{cc}^0$, unchanged. This process leads to a decreasing in size of an inversion window by raising its lower border. Note that γ_{cb}^{ph} produces the same effect on the Rabi oscillations, and hence the decay curves (3) and (4) are close to each other.

Curves (5) and (6) in Fig. 9 show the dependence of pulse energy on the relaxation rates for the two-level system with the same value of cooperative frequency. The decay of the upper state [see curve (5)] results in a very similarly abrupt termination of SF as for the three-level model [compare to curves (1) and (3)]. However, for the two-level system the dephasing process alone [see curve (6)] produces a less pronounced effect [compare to curve (2)]. The faster decay in the three-level configuration can be associated with the additional decay channel—the relaxation of the two-photon coherence γ_{ac}^{ph} (in the example we put $\gamma_{ac}^{ph}=\gamma_{ab}^{ph}$). This decay channel does not appear in a two-level system for obvious reasons. The relaxation γ_{ac}^{ph} destroys the correlation between the driving and probe fields, and, hence, additionally contributes to the energy damping.

VIII. CONCLUSIONS

We have studied the SF effect in a coherently driven V-type medium, and shown that the collective spontaneous emission is possible even with a minor population of the upper SF state ($|a\rangle$ in our notations). Two necessary conditions are to be fulfilled to achieve a SF regime: (i) the initial Raman inversion between two upper states, $|a\rangle$ and $|c\rangle$; (ii) a growth rate of a SF larger than all relaxation rates of the medium.

The developed analytical treatment is based on the assumption that a coherent driving field is strong, i.e., the Rabi frequency of a driving field remains larger than that of a SF pulse for all stages of evolution. This assumption allows us to consider the SF phenomenon in a wide range of parameters in terms of the familiar Maxwell-Bloch formalism that describes the effective two-level system. The shape of a SF pulse is perfectly described in terms of a slowly-varying envelope function filled with fast oscillations. The latter are associated with Rabi floppings on the driving transition, and the envelope is just a solution of the corresponding Maxwell-Bloch equations.

These Rabi floppings periodically produce windows of bare inversion, $\rho_{aa}-\rho_{bb}>0$. The polarization on a SF transition builds up in those time intervals when $\rho_{aa}-\rho_{bb}$ reaches its maximum, and becomes close to zero during the intervals of maximal absorption. In the average, i.e., after integrating over a period of Rabi oscillations, the populations of the states satisfy the LWI condition (72), so that the phenomenon may be called ''superfluorescence without inversion'' by analogy with lasing without inversion.

ACKNOWLEDGMENTS

The authors are pleased to acknowledge a fruitful discussion with Professor J.H. Eberly. The work was supported by the ONR, NSF, U.S. Air Force, and the Welch Foundation. V.K. is also grateful for the support from the Grant Center of Natural Sciences (St. Petersburg, Russia) and the Laser Center of St. Petersburg University. Yuri Rostovtsev thanks the North Atlantic Treaty Organization for its support.

[1] O. Kocharovskaya, Phys. Rep. **219**, 175 (1992); M. O. Scully, *ibid.* **219**, 191 (1992); S. E. Harris, Phys. Today **50** (7), 36 (1997).

[2] R. H. Dicke, Phys. Rev. **93**, 99 (1954).

[3] M. Gross and S. Haroche, Phys. Rep. **93**, 301 (1982).

[4] A. Grubellier, S. Liberman, D. Pavolini, and P. Pillet, J. Phys. B **18**, 3811 (1985); D. Pavolini, A. Grubellier, P. Pillet, L. Cabaret, and S. Liberman, Phys. Rev. Lett. **54**, 1917 (1985).

[5] C. H. Keitel, M. O. Scully, and G. Sussmann, Phys. Rev. A **45**, 3242 (1992).

[6] V. S. Pivtsov, S. G. Rautian, V. P. Safonov, C. G. Folin, and B. M. Chernobrod, Pis'ma Zh. Éksp. Teor. Fiz. **30**, 342 (1979) [JETP Lett. **30**, 317 (1979)]; S. G. Rautian, V. P. Safonov, and B. M. Chernobrod, Izv. Akad. Nauk SSSR, Ser. Fiz. **50**, 640 (1986)[Bull. Acad. Sci. USSR, Phys. Ser. **50**, 14 (1986)].

[7] S. G. Rautian and B. M. Chernobrod, Zh. Éksp. Teor. Fiz. **72**, 1342 (1977) [Sov. Phys. JETP **49**, 705 (1977)]; V. I. Emelyanov and V. N. Seminogov, *ibid.* **76**, 34 (1979) [*ibid.* **49**, 17 (1979)].

[8] E. D. Trifonov, A. S. Troshin, and N. I. Shamrov, Opt. Spectrosk. **48**, 1036 (1980) [Opt. Spectrosc. **48**, 567 (1980)].

[9] V. A. Malyshev, I. V. Ryzhov, E. D. Trifonov, and A. I. Zaitsev, Laser Phys. **8**, 494 (1998).

[10] R. H. Dicke, in *Proceedings of the Third International Conference on Quantum Electronics*, Paris, 1963, edited by P. Grivet and N. Bloembergen (Columbia University Press, New York, 1964), p. 35.

[11] N. Skribanowitz, I. P. Herman, J. C. MacGillivray, and M. S. Feld, Phys. Rev. Lett. **30**, 309 (1973); I. P. Herman, J. C. MacGillivray, N. Skribanowitz, and M. S. Feld, in *Laser Spectroscopy*, edited by R. G. Brewer and A. Mooradian (Plenum, New York, 1974).

[12] J. C. MacGillivray and M. S. Feld, Phys. Rev. A **14**, 1169 (1976); M. F. H. Schuurmans, Q. H. F. Vrehen, D. Polder, and H. M. Gibbs, Adv. At. Mol. Phys. **17**, 167 (1978).

[13] R. Bonifacio, Phys. Rev. A **3**, 512 (1970); **12**, 587 (1975); R. Bonifacio and L. A. Lugiato, Opt. Commun. **47**, 79 (1983).

[14] The semiclassical approach for a two-level SF is discussed in D. C. Burnham and R. Y. Chiao, Phys. Rev. **188**, 667 (1969); R. Friedberg and S. R. Hartman, Phys. Lett. **38A**, 227 (1972); F. T. Arecchi and E. Courtens, Phys. Rev. A **2**, 1730 (1970); R. Saunders, S. S. Hassan, and R. K. Bullough, J. Phys. A **9**, 1725 (1976).

[15] N. E. Rehler and J. H. Eberly, Phys. Rev. A **3**, 1735 (1971).

[16] V. V. Kocharovskii and V. V. Kocharovskii, Usp. Fiz. Nauk **159**, 193 (1989) [Sov. Phys. Usp. **32**, 835 (1989)]; *Cooperative Effects in Matter and Radiation*, edited by C. M. Bowden, D. W. Howgate, and H. R. Robl (Plenum Press, New York, 1977); A. V. Andreev, V. I. Emel'yanov, and Yu. A. Il'inskii, *Cooperative Effects in Optics. Superfluorescense and Phase Transitions* (Institute of Physics Publishing, London, 1993); M. G. Benedict, A. M. Ermolaev, V. A. Malyshev, I. V. Sokolov, and E. D. Trifonov, *Super-radiance, Multiatomic Coherent Emission* (Institute of Physics Publishing, London, 1996).

[17] R. Bonifacio, D. M. Kim, and M. O. Scully, Phys. Rev. **187**, 441 (1969).